Available online at www.sciencedirect.com
ScienceDirect
Clinical Biomechanics 22 (2007) 230–238
CLINICAL BIOMECHANICS
www.elsevier.com/locate/clinbiomech

An investigation into the deformable characteristics of the human foot using fluoroscopic imaging

N. Wrbaškić, J.J. Dowling *

Department of Kinesiology, McMaster University, 1280 Main Street West, Hamilton, ON, Canada L8S 4K1

Received 20 January 2006; accepted 19 September 2006

Abstract

Background. To determine the behaviour of the human foot during *in vivo* loading and unloading.

Methods. Fluoroscopic imaging was used to investigate the movement of the bones and 13 skin markers during loading and unloading for the medial aspect of the left foot. A foot-pressure measuring system was compared with a force plate used to gather kinetic information, simultaneously. Four male and two female subjects performed three tasks that mimicked jumping, walking, and sprinting. Two-dimensional vector displacements were calculated between bone landmarks over time. Foot rigidity was assessed by a 5 mm length variability threshold determined as the difference between the third and first quartiles of the data set.

Findings. The displacement between the first metatarso-phalangeal joint and distal aspect of the calcaneous varied more than the 5 mm threshold. A new foot model was developed which included three rigid segments joined together by hinge joints located at the first metatarso-phalangeal joint and between the anterior talus and navicular. The comparison between skin mounted markers and bone landmarks yielded a range of correlation slopes close to 1.00 for both the x- and y-directions. Foot pressure and force plate comparisons were promising ($\%RMS_{error} \sim 10\%$) for the vertical ground reaction forces but not so for the centres of pressure ($\%RMS_{error}$ up to 50%).

Interpretation. A multi-segment foot model is required to better represent the behaviour of a human foot. No consistent skin marker movement was determined. Better pressure distribution devices need to be developed to determine more accurate foot kinetics. Precise foot kinematics are required in order that accurate ankle moments and reaction forces be determined for the purpose of assessing foot and ankle function.

Keywords: Gait analysis; Foot loading; Model

1. Introduction

When performing mechanical energy and power calculations for the thigh, leg and foot during walking and running, the human foot has traditionally been modelled as a rigid triangle joined to the leg by a fixed hinge joint (Robertson and Winter, 1980; Caldwell and Forrester, 1992). The ankle joint, the metatarso-phalangeal joint and the heel define each vertex of this triangular foot. The great toe was not included in this model of the foot as a result of the plantar- and dorsiflexion that can occur at the metatarso-phalangeal joint (Winter, 1983). A single vector acting at the centre of pressure typically represented the distribution of force underneath the foot when the foot was in contact with the ground.

This model has allowed for the use of inverse dynamics of a rigid link system (foot, leg, thigh, etc.) so that internal forces could be estimated. In order to validate these forces and moments, the total segment power has been compared to the rate of change of mechanical energy (Robertson and Winter, 1980; Siegel et al., 1996) as the two have theoretically been shown to be equal for any rigid segment (Aleshinsky, 1986; van Ingen Schenau and Cavanagh, 1990).

* Corresponding author.
E-mail addresses: nwrbaskic@hotmail.com (N. Wrbaškić), dowlingj@mcmaster.ca (J.J. Dowling).

0268-0033/$ - see front matter © 2006 Elsevier Ltd. All rights reserved.
doi:10.1016/j.clinbiomech.2006.09.006

In practice, this relationship has been verified for the thigh, leg and foot segments for the recovery phase of sprinting (Vardaxis and Hoshizaki, 1989), for the thigh and leg segments for all aspects of the gait cycle and for the foot during the swing phase but not during weight acceptance and the late push-off phase of the gait cycle (Robertson and Winter, 1980; Quanbury et al., 1975). The explanation put forth as to the reason why a poor agreement exists between total segment power and rate of change of energy for the foot during the stance phase has been either experimental error and/or a violation of the link-segment modelling assumptions.

It has been demonstrated by de Looze et al. (1992) that constant segment length is of great importance to the calculation of total segment power. Modelling the foot without any toes, without any joints distal to the ankle, without the inclusion of any viscoelastic tissue on the plantar aspect of the foot, nor any spatial characteristics in the mediolateral axis has been a general criticism of existing models (Scott and Winter, 1993). All or part of the aforementioned reasons may explain the poor relationship between total segment power and rate of change of energy for the foot during weight bearing activities.

Siegel et al. (1996) improved the match between the total segment power and rate of change of energy for the foot during the stance phase of gait by introducing a distal foot power term that accounted for the movement of the joints within the foot and the compression of the plantar fat pads that would likely produce a non-zero distal foot velocity. However, their method does not distinguish between passive tissue viscoelasticity and/or the possible metatarsophalangeal muscle power which could be part of their distal power term. If the metatarso-phalangeal muscle power is included in the distal power term, then it would not have been part of the calculation of the moment at the ankle and thus would be missing from the subsequent calculations at the knee and hip.

The foot has been shown to behave as both an arch or truss and as a beam (Hicks, 1955). Also, it has been proposed that the foot acts as a shock absorbing structure to dampen the forces that exist during initial contact with the ground when walking, running, and jumping (Alexander, 1987). Initially, Lapidus (1943) argued that the purpose of the longitudinal arch of the foot was to increase the strength of the foot as a lever. The role of the plantar aponeurosis was to act as a cable that could withstand tremendous tensile stress, without any change in length, and thus, could not behave as a spring.

More recently, Wright and Rennels (1964) showed that the arch of the foot elongated during load. Similarly, Ker et al. (1987) demonstrated that the foot can store about 17 J of energy in the compliant elements of the arch of the foot that would make running more energy efficient. This was determined on amputated feet that allowed for horizontal displacement of the heel and ball of the foot. This may not actually happen when the foot contacts the ground due to frictional forces.

Many models of the foot have been developed over the years (Salathé et al., 1986; Scott and Winter, 1993; Kim and Voloshin, 1995), however, there has yet to be a study that has investigated the nature of the bones of the human foot during load bearing in an *in vivo* situation. Fluoroscopic imaging allows us to capture, on video, real-time motion of internal structures within the human body as in the human heel pad (De Clercq et al., 1994).

Can the foot, when placed under load *in vivo*, be modelled as a single rigid structure, or as multiple rigid segments linked together? In order to determine this, fluoroscopic imaging technology was used. If indeed, the foot can only be accurately represented as multiple rigid segments, then determining the external ground reaction forces under each segment would be necessary. Current inverse dynamics use a force plate but this is only capable of resolving the ground reaction forces into a single resultant.

Research, by Hayafune et al. (1999), into the pressure and force patterns under the foot has shown that the great toe has the highest peak values for pressure during the push-off phase in gait. Furthermore, Jacob (2001) used pressure distribution data along with anthropometric information from cadaver feet to estimate the internal forces in the forefoot during normal gait. There has yet to be a study that investigated the movements of the bones within the foot during *in vivo* loading and unloading.

The purposes of the present investigation were to (1) develop a foot model based upon actual two-dimensional (2D) movements of the bones within the foot in the sagittal plane during *in vivo* loading and unloading, (2) determine how accurately skin markers can reflect the actual bone movements, and (3) determine the efficacy of using a multi-component pressure-sensing device, such as F-Scan, in the case a multi-segment foot model is warranted.

2. Methods

2.1. Subjects

Six university students (4 male and 2 female) volunteered to participate in the study. Table 1 lists the characteristics of the subjects. Verbal and written instructions about the protocol of the experiment were given to all participants, each of whom signed an informed consent form prior to his/her involvement in the study. This investigation was approved by the President's Committee on Ethics of Research on Human Subjects at McMaster University.

Table 1
Subject characteristics

Parameter	Males Mean (SD)	Females Mean (SD)
Age (yr)	25.3 (2.1)	24.5 (0.7)
Height (cm)	176.3 (2.1)	151.2 (1.7)
Total body mass (kg)	73.9 (5.4)	47.3 (2.5)

SD – standard deviation; yr = year.

2.2. Experimental setup

The setup for this experiment incorporated several pieces of equipment for measuring both kinematic and kinetic variables. Fluoroscopy imaging technology (Polystar T.O.P. – Model Fluorospot, Siemens, Erlangen, Germany) was employed to observe the motion of the bones of the foot and externally placed markers while subjects performed several different tasks. A pressure-sensing sheet (F-Scan – version 3.623, Tekscan Inc., Boston, USA) was used to measure the distribution of pressure under the foot. This ultra-thin (0.007 in.) flexible printed circuit consisted of 960 individual pressure-sensing cells and was outlined in the shape of a left foot. The centre of each pressure-sensing cell was located 0.508 cm (0.2 in.) from that of the adjacent one. The effective sensor area for each cell was 0.258064 cm^2 (0.04 $in.^2$).

The F-Scan sheet was taped to the top of a multi-component strain-gauge force plate (AMTI model OR65, Advanced Mechanical Technology, Inc., Watertown, Massachusetts, USA). The force plate is typically used to measure the ground reaction forces and moments when subjects make contact with it during walking, running or jumping. The force plate was mounted on a wooden platform that was built for this experiment. The wooden platform, which measured 65.4 cm (25.75 in.) in height, was necessary in order to raise the force plate off of the ground since the X-ray emitter of the fluoroscopy unit was not capable of being positioned near the ground.

2.3. Experimental protocol

Height and total body mass were recorded for each subject. Additionally, the weight of each subject was recorded while they were wearing a lead jacket and collar which was necessary while they were being scanned by the fluoroscopy unit.

Thirteen skin markers containing ball bearings (one-eighth of an inch or 0.3175 cm in diameter) were placed on the following landmarks on the medial side of the left foot (see Fig. 1): (1) distal aspect of the hallux, (2) interphalangeal joint of the great toe (hallux), (3) the first metatarso-phalangeal (1mp) joint, (4) the best estimate, after palpation, the first metatarso-tarsal joint (first metatarso-medial cuneiform joint), (5) between the medial cuneiform and the navicular, (6) the anterior and (7) posterior aspects of the talus which were determined by palpation when each subject everted their left foot, (8) the posterior aspect of the heel where the Achilles tendon inserts, (9) the distal part of the heel (at the heel pad), (10) this marker was placed proximal and anterior to the heel pad and in line with marker nine, (11) the distal part of the medial malleolus, and two markers were placed slightly above the medial malleolus, (12) one anterior and (13) the other posterior. The skin markers were placed as close to the actual bone landmarks as possible.

There were three tasks that the subjects were asked to perform all beginning the same way. The subjects stood on their right foot to one side of the force plate while their

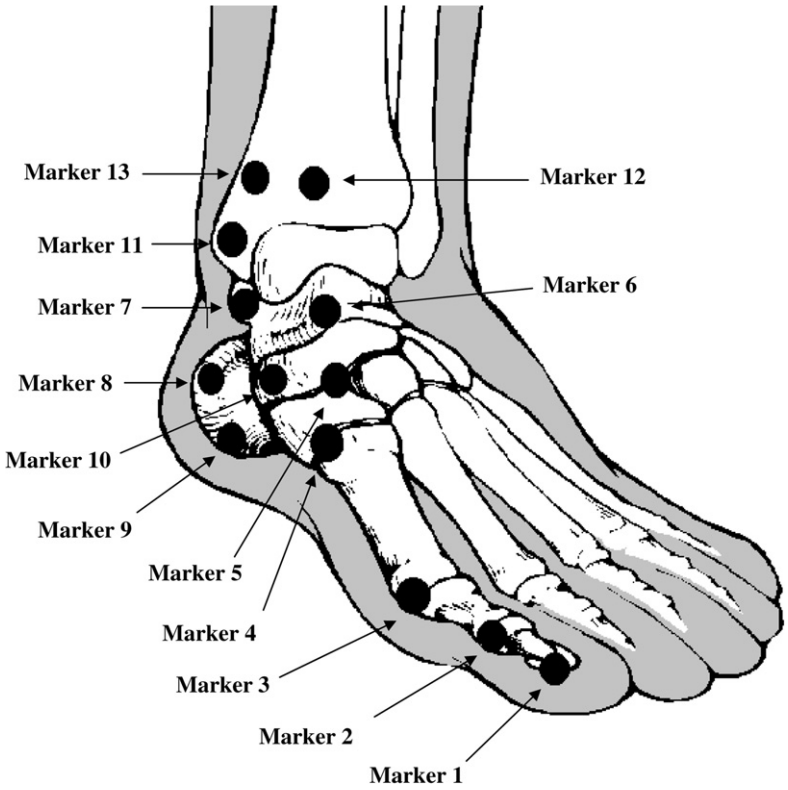

Fig. 1. Skin marker placement.

left foot was positioned above the force plate but not in contact with it. Upon commencement of each task, the left foot of each subject was lowered onto the F-Scan pressure-sensing sheet, which was taped to the top of the force platform, while their right foot was raised off of the wooden platform as they transferred their weight onto their left foot.

At this point, the subjects performed one of three slightly different tasks. The first task (referred to as the "jump" task) required the subjects to perform a vertical jump off of their left foot. Their hands were positioned on their hips during the "jump" task and the subjects were allowed to land on both feet. The second task, which will be referred to as the "lift" task, required the subjects to lift themselves onto their toes and then lower their heel back onto the pressure sensors. For the third task, the participants were requested to contact the pressure sensors only with their toes and the ball of their left foot. This task will be referred to as the "toes" task. The "jump", "lift" and "toes" tasks were chosen in an attempt to mimic jumping, walking and running, respectively.

2.4. Data collection

During the trials, the subjects were exposed to a negligible amount of radiation. The fluoroscopy technique had a source to image distance of 1.15 m at 60 kVp and 0.4 mA for a maximum of 8 s. The measured exposure rate was 43 mR per minute which resulted in 5.7 mR for the 8 s. The average person is exposed to approximately 200 mR (more than 35 times the measured amount) from sources such as the sun and television in a typical year.

The images that were scanned by the fluoroscopy unit were recorded on video by a Panasonic (AG-7350) video cassette recorder at a scanning rate of 30 frames per second. The Peak5 Motion Measurement System (Peak Performance Technologies Inc., Englewood, USA) was used to manually digitize the movements of both the bones and skin markers. The data were digitized at a frame rate of 60 Hz since the Peak5 system separated each video recorded frame into two different fields of alternating raster lines. The missing raster lines in each field were then interpolated by Peak5 to, in essence, yield two digitizing frames from one recorded frame. Both the force plate and F-Scan pressure sensor sampled data at 90 Hz.

The F-Scan pressure sensor was calibrated with the force plate for every subject. This was accomplished by having each person stand on the F-Scan pressure-sensing sheet which was taped to the top of the force plate while measuring the individual's total body weight.

2.5. Data processing

Foot bending was determined by way of vector displacements of the skin marker and bone data calculated in the sagittal plane. Cubic spline estimation was used to interpolate any missing skin marker or bone data after the digitization process. The positional data were then filtered using a dual-pass, critically damped, low-pass filter with a cut-off frequency of 15 Hz. Custom software was developed for the calculation, display, and comparison of the vertical ground reaction forces and centres of pressure for the F-Scan with the force platform.

2.6. Model development

The determination of foot deflection under load began with the definition of the traditional foot, used for rigid link-segment modelling, which represents the foot as a rigid triangle defined by the ankle joint, the metatarso-phalangeal joint and the heel. Subsequent calculations for segment lengths were performed whereby the number of segments increased as the segment lengths decreased. This was done in an attempt to develop the most simplistic foot model as possible that would meet the criteria for the use of traditional link-segment mechanics.

There were difficulties in analyzing the ankle complex since digital information was lost during the digitization process. Skin markers 11, 12, and 13, as well as the bone landmark equivalents, fell into this category. A possible explanation may be that the density of bone in this area (ankle complex) may be more than at other parts of the foot and therefore, the contrast between the skin markers and the bones was very small. Due to the problems of digitizing the ankle, the analysis was limited to the talus and inferior structures.

2.7. Data analysis

The following equation was used to calculate the lengths between bone landmarks:

$$\mathrm{SL} = \sqrt{(x_i - x_j)^2 + (y_i - y_j)^2} \quad (1)$$

where SL – segment length; i, j represent the number for the bone landmark and $i \neq j$.

Segment lengths, between any two bone landmarks over time, were then ordered from the shortest to the longest lengths and the difference between the third and first quartile values was used as the measure for segment length variability. This was done so that extraneous values in the data set, as a result of digitizing errors or filtering anomalies, would be eliminated and therefore would not skew the results. A difference of 5 mm between the third and first quartile values was chosen as the threshold for the determination of segment rigidity. A value less than 5 mm meant the segment was rigid and a difference score of more than 5 mm deemed that the two bone landmarks were not rigidly attached. This 5 mm threshold is based on the human variability of manual digitization of a stationary object of known length after being scanned by the fluoroscopy unit and recorded on video tape.

For instance, if the lengths between bone landmarks 3 (first metatarso-phalangeal joint) and 9 (the distal part of

the heel) (see Fig. 1) were compared over time, this segment would be considered rigid if the segment lengths did not vary more than 5 mm between the third and first quartiles of the data set. If, on the other hand, this segment's length changed more than 5 mm, then it would not be considered rigid.

The relationship between the skin marker movement and actual bone movement was assessed by looking at the slopes of the regression lines for position versus time in both the *x*- and *y*-directions. The positive direction of the *x*-axis was defined as a horizontal line heading in the anterior direction while a vertical line moving in the superior direction defined the positive *y*-axis. Pearson product-moment correlations (*r*) were used to correlate the F-Scan and force plate data while root mean square error (RMS_{error}) and percent root mean square error ($\%RMS_{error}$) were used to assess the magnitude of the discrepancy between the data sets. $\%RMS_{error}$ was expressed as a percentage of the force plate data. The *x*-direction for the centre of pressure data was consistent with that of the marker axis system described above.

3. Results

3.1. Model development

Fig. 2 illustrates the results of the variability of the distances between the bone landmarks. It is clearly seen that the length between the anterior talus and the heel, indicated by the segment 6–9, did not exceed the 5 mm threshold for any of the tasks. Thus, this segment can be considered to be rigid.

This is also true, for the most part, for segment 3–6 (1mp to anterior talus). Even though the length of the bone landmarks for the jump trial was slightly over the 5 mm threshold, those same bone landmarks were well below the threshold for both the lift and toes trials. Therefore, the segment defined as the distance between the anterior talus and the 1mp joint can be considered rigid as well.

The last test for the use of the traditional triangular foot was the length between the 1mp and heel defined as the segment 3–9 in Fig. 2. In this case, the test failed as the variability in length between these bone landmarks was above the 5 mm threshold for all of the tasks, namely the "jump", "lift" and "toes" tasks. An analysis of the length between the distal aspect of the great toe and the anterior aspect of the talus over time (segment 1–6) was performed to see whether a rigid segment could be defined between these two points. Fig. 2 shows that these two points exceed the 5 mm variability threshold and therefore cannot be rigidly attached. These results prompted the development of a new foot model based on the observations made from fluoroscopic imaging of the actual movements of the bones of the foot (see Fig. 3).

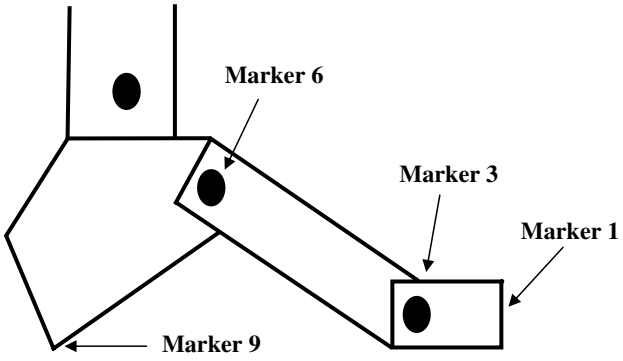

Fig. 3. New foot model.

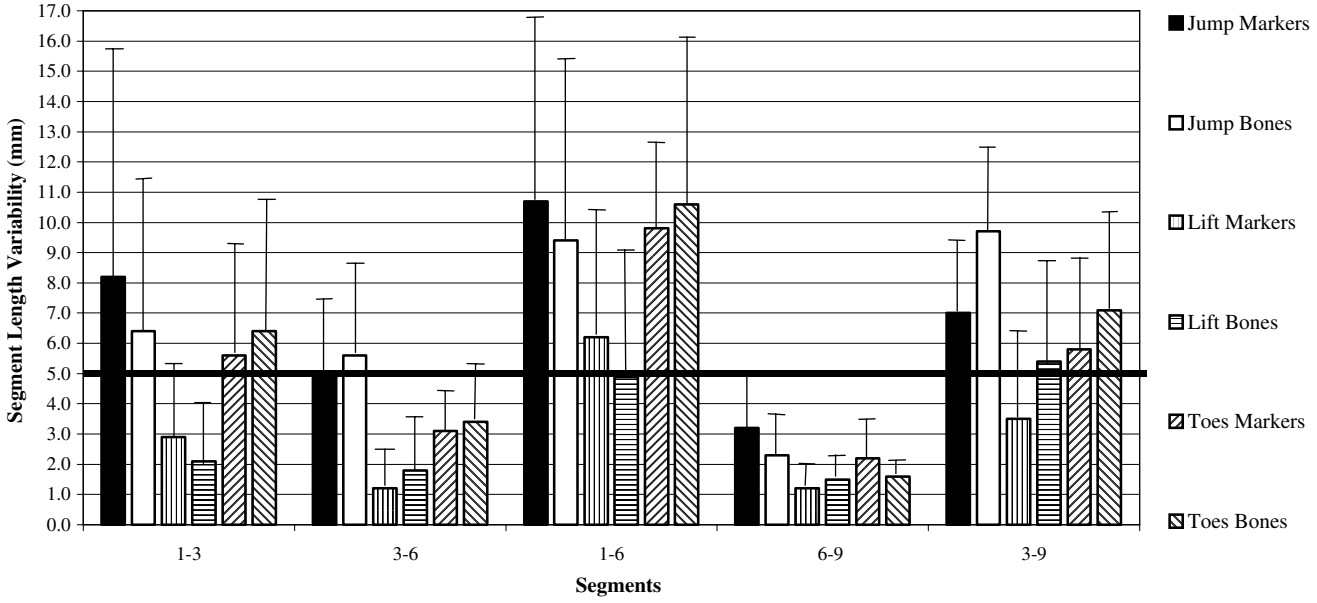

Fig. 2. Mean variability of segment lengths determined as the difference between the third and first quartiles of the data set. Refer to Fig. 1 for a diagram of marker placements. Error bars indicate 1 standard deviation.

Table 2
Mean correlation slopes, SD and r values of skin marker (M) and bone landmark (B) movement for each task ($n = 6$)

	Jump			Lift			Toes		
	Mean	SD	r	Mean	SD	r	Mean	SD	r
Mx1–Bx1	0.90	0.13	0.913	1.06	0.14	0.970	0.82	0.17	0.536
My1–B1	1.07	0.06	0.995	1.07	0.02	0.995	1.04	0.09	0.964
Mx3–Bx3	0.76	0.21	0.921	0.80	0.12	0.980	1.07	0.09	0.865
My3–By3	1.07	0.22	0.836	1.06	0.08	0.977	1.07	0.11	0.948
Mx6–Bx6	0.99	0.21	0.904	1.01	0.05	0.995	1.07	0.09	0.974
My6–By6	0.86	0.48	0.793	1.28	0.09	0.967	1.09	0.34	0.804
Mx9–Bx9	0.86	0.21	0.871	1.17	0.15	0.982	1.13	0.14	0.981
My9–By9	1.15	0.22	0.804	1.07	0.04	0.997	1.04	0.06	0.997

x – x-direction; y – y-direction; numbers – marker location according to Fig. 1.

3.2. Skin marker and bone comparison

Table 2 displays the data of the comparisons for the skin marker and bone equivalents in both the x- and y-directions. Marker movements seem to reflect bone movements based upon the high correlation coefficients. The fact that most of the slopes linger around a value of one indicates that there is a one-to-one relationship in the movement patterns between the two variables. Only markers 1, 3, 6, and 9 were compared as these markers define the segments of the new proposed foot model.

3.3. F-Scan and force plate comparison

Statistics for the comparison between the vertical ground reaction forces (F_y) and the centres of pressure in the x-direction ($CofP_x$) between the F-Scan and the force plate can be seen as given in Tables 3 and 4, respectively. An excellent agreement exists between the two force recording instruments for the variable F_y.

As in the case with F_y, there is a good correlation between F-Scan and the force plate for $CofP_x$. There is, however, a difference in the magnitude of the two curves as shown in the RMS_{error} scores. Randomly selected curve comparisons between F-Scan and force plate for F_y and $CofP_x$ values are depicted in Fig. 4 for the "jump", "lift", and "toes" tasks.

Table 3
Means (SD) for F_y between F-Scan and force plate ($n = 6$)

Task	Jump	Lift	Toes
r	0.998 (0.000)	0.992 (0.004)	0.996 (0.002)
RMS_{error} (N)	29.10 (11.33)	36.90 (8.17)	31.16 (7.96)
$\%RMS_{error}$	6.95% (1.92)	12.88% (3.47)	10.23% (2.38)

Table 4
Means (SD) for $CofP_x$ between F-Scan and force plate ($n = 6$)

Task	Jump	Lift	Toes
r	0.883 (0.077)	0.958 (0.021)	0.941 (0.016)
RMS_{error} (m)	0.049 (0.014)	0.027 (0.006)	0.037 (0.009)
$\%RMS_{error}$	49.52% (13.22)	32.52% (8.73)	34.91% (4.72)

4. Discussion

In the area of human locomotion research, the most poorly modelled aspect of the lower appendage has been the foot in terms of its interaction with the environment (Scott and Winter, 1993). In order to develop a more accurate model of the foot during loading and unloading, accurate kinematic information is required. Making use of the fluoroscopic imaging technology has enabled us to observe the actual movements of the bones within the living human foot during dynamic loading and unloading. Fig. 2 shows which parts of the foot remained rigid and which parts did not during the "jump", "lift", and "toes" tasks. Foot rigidity was maintained between the anterior talus and the distal aspect of the calcaneous and between the anterior talus and the first metatarso-phalangeal (1mp) joint in this 2D, sagittal plane investigation. It should be noted that there may well be motion at the subtalar joint, as its axis is oblique, which may not have been observed in the sagittal plane. The distance between the 1mp joint and the distal aspect of the calcaneous varied more than the 5 mm threshold and thus was considered not to be rigid. This coincides with work done on amputated feet by Ker et al. (1987) and by way of a mathematical model developed by Kim and Voloshin (1995).

Performing rigid link-segment mechanics on the foot which deforms under load, can yield conclusions about its behaviour that are suspect. This was confirmed by the fact that power estimates were not verified for the foot for the stance phase of walking (Robertson and Winter, 1980). Furthermore, it is understandable why power estimates were validated for the foot during the swing phase of walking and running when it is modelled to be rigid since the external forces acting on the foot during this phase would be quite small and would not cause it to deform and change length. Recently, Buczek et al. (2006) showed that joint powers could account for the discrepancy observed between an inverted pendulum model applied to human gait and actual force traces recorded during single support. These authors also reported the need to analyze gait patterns of a more demanding nature that would be associated with changes in joint powers. Thus, determining accurate joints powers will be critical in such analyses.

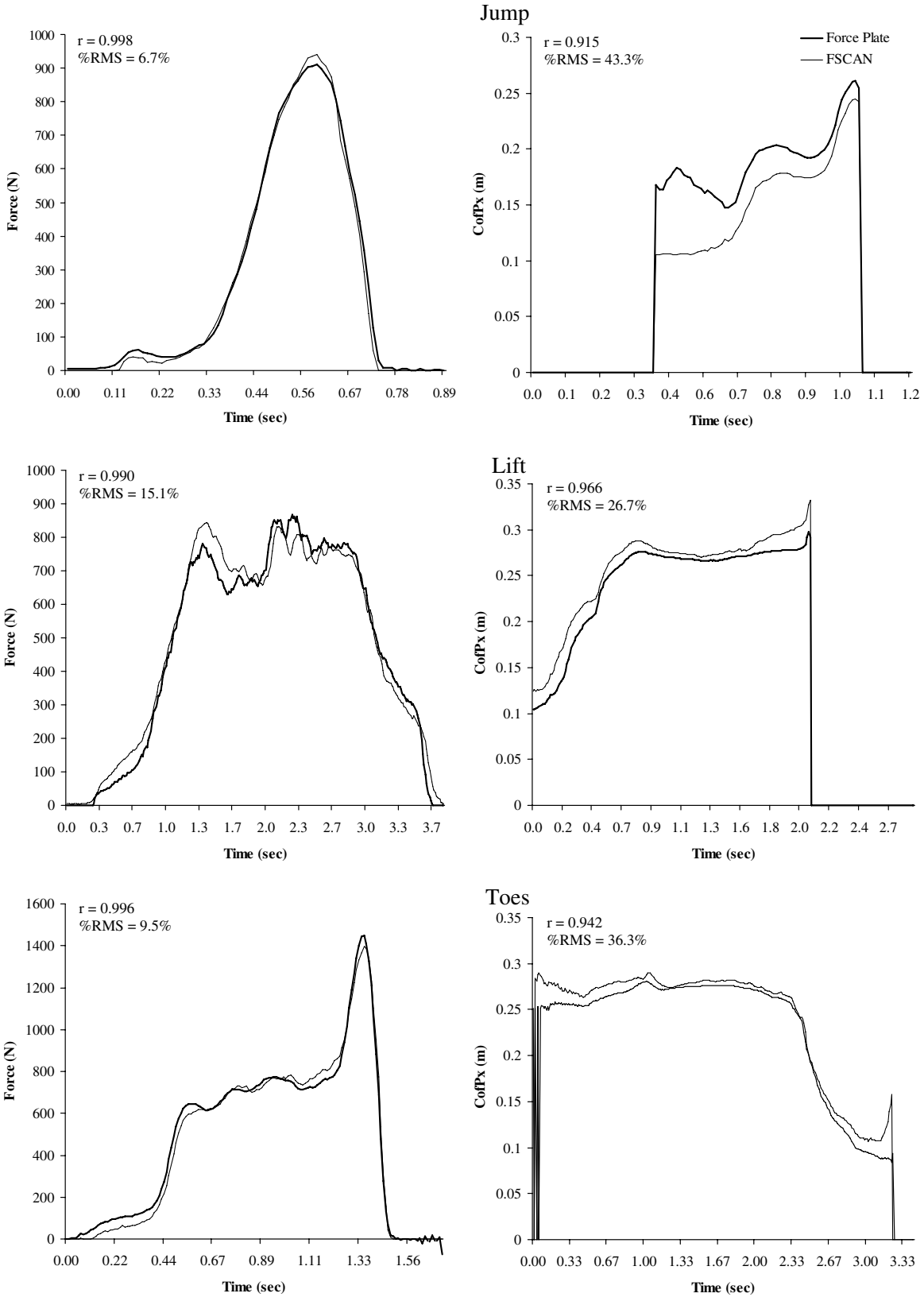

Fig. 4. Randomly selected graphs of the comparison between the F-Scan and force plate for F_y and CofP$_x$ for the "jump", "lift" and "toes" trials.

Based on the data, a new foot model has been developed (Fig. 3). Hinge joints were necessary at the anterior talus and at the 1mp joint. The toe segment was modelled as one rigid segment even though the data was somewhat

ambiguous to its state of rigidity when in contact with the ground. It appeared that some subjects curled their toes while others did not. Therefore, there could be different strategies employed by different people in order to stabilize the inter-phalangeal joint. Jacob (2001) demonstrated the importance of stabilizing the inter-phalangeal joint during gait in that it has to enable transmitting the maximum measured 45% body weight from under the great toe as reported by Hayafune et al. (1999).

It was unfortunate that the ankle was not able to be analyzed due to loss of digital information during the digitization process. Whether the ankle can be modelled as a true hinge joint needs to be investigated in future studies as this will affect the way reaction forces and moments are calculated at the ankle.

To substantiate the findings, a comparison was made between skin marker movement and the actual bone movement. Tranberg and Karlsson (1998) used 2D roentgen photogrammetry to study the relative movement of the skin markers and underlying bony structures during three static positions. They found that the more proximally placed skin markers (around the ankle) produced greater deviations from the underlying bony structures than did the more distally placed markers. The present study showed that there were markers that departed from a correlation slope of 1.00 with or without having a relatively high standard deviation. There seems to be no consistent pattern of marker movement with respect to the bony structures across the different tasks.

The necessity of using a multi-segment foot model, as the one advocated in this paper, warrants the use of a device capable of yielding the distribution of force on the plantar surface of the foot since a single centre of pressure vector, traditionally given by a force plate, is no longer sufficient. An F-Scan pressure-sensing sheet was used as such a device. The F-Scan sheet was taped to the top of the force plate so that vertical ground reaction force (F_y) and centre of pressure (CofP_x) information could simultaneously be recorded by both instruments. F-Scan cannot measure F_x or F_z and this may be a limitation for its use in walking and running or other movements with non-trivial shear forces.

The correlation coefficients were above 0.99 for F_y while the $\%\mathrm{RMS}_{\mathrm{error}}$ was around 10% for each of the tasks. Slightly lower r-values were observed for the CofP_x between the F-Scan and force plate. The $\%\mathrm{RMS}_{\mathrm{error}}$, on the other hand, was not as favourable as for the F_y since the discrepancies were above 30%. These discrepancies relate to a minimum CofP_x difference of 2.7 cm (mean for "lift" trial). This raises some concern as to the accuracy of the F-Scan under the assumption that the force plate is the more accurate of the two devices. There may be some calibration problems with each individual pressure-sensing cell of the F-Scan which may explain the good agreement in F_y but not in CofP_x between the two instruments. As the F-Scan is based on a resistive-type sensor, it has been stated that the reproducibility of these types of sensors is relatively poor (Schaff, 1993).

5. Conclusions

This study showed that the traditional rigid triangular foot can no longer be used to model the true behaviour of the human foot under load bearing conditions. This investigation was unable to describe the true motion of the ankle due to the loss of digital information during the digitization process and thus, future studies need to address this issue as it is pertinent in calculating accurate kinetics at the ankle. There is also a need to record fluoroscopic images at a higher rate so that the motion of the bones can be clearly observed at higher velocities. These suggestions will give researchers more insight into the true behaviour of the human foot. This information can then be used to develop better foot orthotics, create better foot and leg prosthetics, improve athletic performance, prevent injuries of the foot and leg and produce better shoes for both athletic and leisure purposes.

Additionally, this study showed that there is movement of the skin mounted markers as compared to the underlying bony structures as reflected in the slopes of the correlation regression lines. Furthermore, the accuracy of the F-Scan foot pressure sensor needs to improve so that foot energetics may be better determined since multiple resultant reaction forces and their points of application are required. Determining accurate reaction forces and moments *within the foot* is critical as these values are used for subsequent calculations at the knee which in turn are used at the hip. Until such a valid and reliable pressure-sensing device is built, our understanding of the internal causes of movement and the influence of external forces on the human body may not be fully understood.

Acknowledgements

The authors would like to thank John Moroz for all of his technical support and Eric Bapty for his assistance during data collection and the use of his F-Scan system. Additionally, appreciation goes out to Bridget Brown and Sheila Hagel for their time and assistance with the fluoroscopy scanner.

References

Aleshinsky, S.Y., 1986. An energy 'sources' and 'fractions' approach to the mechanical energy problem – I. Basic concepts, description of the model, analysis of a one link system movement. Journal of Biomechanics 19, 287–293.

Alexander, R.McN., 1987. The spring in your step: the role of elastic mechanisms in human running. In: de Groot, G. et al. (Eds.), Biomechanics XI. Free University Press, Amsterdam, pp. 12–17.

Buczek, F.L., Cooney, K.M., Walker, M.R., Rainbow, M.J., Concha, M.C., Sanders, J.O., 2006. Performance of an inverted pendulum model directly applied to normal gait. Clinical Biomechanics 21, 288–296.

Caldwell, G.E., Forrester, L.W., 1992. Estimates of mechanical work and energy transfers: demonstration of a rigid body power model of the recovery leg in gait. Medicine and Science in Sports and Exercise 24 (10), 1396–1412.

De Clercq, D., Aerts, P., Kunnen, M., 1994. The mechanical characteristics of the human heel pad during foot strike in running: an *in vivo* cineradiographic study. Journal of Biomechanics 27, 1213–1222.

de Looze, M.P., Bussmann, J.B.J., Kingma, I., Toussaint, H.M., 1992. Different methods to estimate total power and its components during lifting. Journal of Biomechanics 25, 1089–1095.

Hayafune, N., Hayafune, Y., Jacob, H.A.C., 1999. Pressure and force distribution characteristics under the normal foot during the push-off phase in gait. The Foot 9, 88–92.

Hicks, J.H., 1955. The foot as a support. Acta Anatomica 25, 34–45.

Jacob, H.A.C., 2001. Forces acting in the forefoot during normal gait – an estimate. Clinical Biomechanics 16, 783–792.

Ker, R.F., Bennett, M.B., Bibby, S.R., Kester, R.C., Alexander, R.McN., 1987. The spring in the arch of the human foot. Nature 325, 147–149.

Kim, W., Voloshin, A.S., 1995. Role of plantar fascia in the load bearing capacity of the human foot. Journal of Biomechanics 28, 1025–1033.

Lapidus, P.W., 1943. Misconception about the "springiness" of the longitudinal arch of the foot. Archives of Surgery 46, 410–421.

Quanbury, A.O., Winter, D.A., Reimer, G.D., 1975. Instantaneous power and power flow in body segments during walking. Journal of Human Movement Studies 1, 59–67.

Robertson, D.G.E., Winter, D.A., 1980. Mechanical energy generation, absorption, and transfer amongst segments during walking. Journal of Biomechanics 13, 845–854.

Salathé Jr., E.P., Arangio, G.A., Salathé, E.P., 1986. A biomechanical model of the foot. Journal of Biomechanics 19, 989–1001.

Schaff, P.S., 1993. An overview of foot pressure measurement systems. Clinics in Podiatric Medicine and Surgery 10, 403–415.

Scott, S.H., Winter, D.A., 1993. Biomechanical model of the human foot: kinematics and kinetics during the stance phase of walking. Journal of Biomechanics 26, 1091–1104.

Siegel, K.L., Kepple, T.M., Caldwell, G.E., 1996. Improved agreement of foot segmental power and rate of energy change during gait: inclusion of distal power terms and use of three-dimensional models. Journal of Biomechanics 29, 823–827.

Tranberg, R., Karlsson, D., 1998. The relative skin movement of the foot: a 2-D roentgen photogrammetry study. Clinical Biomechanics 13, 71–76.

van Ingen Schenau, G.J., Cavanagh, P.R., 1990. Power equations in endurance sports. Journal of Biomechanics 23, 865–881.

Vardaxis, V., Hoshizaki, T.B., 1989. Power patterns of the leg during the recovery phase of the sprinting stride for advanced and intermediate sprinters. International Journal of Sport Biomechanics 5, 332–349.

Winter, D.A., 1983. Moments of force and mechanical power in jogging. Journal of Biomechanics 16, 91–97.

Wright, D.G., Rennels, B.S., 1964. A study of the elastic properties of plantar fascia. Journal of Bone and Joint Surgery 46, 482–492.